

Control of a 3-DOF Over-Actuated Parallel Mechanism

Frédéric Marquet, Olivier Company, Sébastien Krut, Olivier Gascuel, François
Pierrot

► **To cite this version:**

Frédéric Marquet, Olivier Company, Sébastien Krut, Olivier Gascuel, François Pierrot. Control of a 3-DOF Over-Actuated Parallel Mechanism. DETC: Design Engineering Technical Conferences - CIE: Computers and Information in Engineering Conference, Sep 2002, Montreal, Canada. pp.458. lirmm-00269419

HAL Id: lirmm-00269419

<https://hal-lirmm.ccsd.cnrs.fr/lirmm-00269419>

Submitted on 3 Apr 2008

HAL is a multi-disciplinary open access archive for the deposit and dissemination of scientific research documents, whether they are published or not. The documents may come from teaching and research institutions in France or abroad, or from public or private research centers.

L'archive ouverte pluridisciplinaire **HAL**, est destinée au dépôt et à la diffusion de documents scientifiques de niveau recherche, publiés ou non, émanant des établissements d'enseignement et de recherche français ou étrangers, des laboratoires publics ou privés.

CONTROL OF A 3-DOF OVER-ACTUATED PARALLEL MECHANISM

Frédéric Marquet Olivier Company

Sébastien Krut Olivier Gascuel François Pierrot

LIRMM - UMR 5506 CNRS / UM2
161, rue Ada - 34392 Montpellier cedex 5, France
URL: www.lirmm.fr/rdc/marquet@lirmm.fr

ABSTRACT

This paper presents the control of ARCHI, a 3-dof over-actuated parallel mechanism, designed as a subpart of a 5-axis hybrid machining robot. Control strategies of the parallel sub-mechanism (3 dof / 4 actuators) managing the internal constraint on the mechanism are proposed and experimental results are discussed.

I. INTRODUCTION

The concept of parallel robots yet demonstrated its efficiency in terms of mechanism stiffness and dynamic performances. At the present time, these robots are used for various applications such as pick-and-place (Delta [1] or H4 [2],[3] robots can reach accelerations higher than 10 g for carrying objects, allowing high production rates), high-speed machining where high stiffness and velocities are essential (for example the Renault Automation 3-dof machining center UraneSx [4] able to reach 3.5 g or Toyoda 6-dof machine-tool HexaM [5]). However, if the efficiency of these machining centers is not to be demonstrated limitations subsist. In fact, on one hand, UraneSx machine has only 3 dof -insufficient to complete all kind of machining tasks- and, on the other hand, 6-dof machines have a limited tilting angle (± 20 degrees orientation capability for the HexaM spindle) that restricts their possibility of use. To overcome these limitations, a solution consists in designing mechanical amplification devices such as Twice [6]. Another solution is to design over-actuated robots that eliminate the singular positions from the workspace. In this

way, relatively few over-actuated parallel robots have been yet studied (however, interesting works concerning the control of a one and a two-dof redundant robots described in [7] and [8] have to be mentioned) . In order to obtain 5-axis machines, a possibility is to design hybrid machines associating a serial to a parallel over-actuated mechanism as proposed by Seoul University with the efficient (but complex) Eclipse machine [9][10].

Combining both concepts, ARCHI robot presented in this paper is a 5-axis hybrid over-actuated machine. The study of the control strategies of the redundant parallel 3-dof sub-mechanism is the aim of this paper. After recalling ARCHI design and modeling, several control strategies managing the internal constraints on the over-actuated robot are presented (“two-arm like” control, minimization of the Euclidian and infinite norm of actuators forces) and tested on a prototype.

II. ARCHI PARALLEL REDUNDANT ROBOT

II.1. ARCHI concept

ARCHI design is depicted in details in [11]. ARCHI robot consists of the association of a hybrid parallel mechanism actuated by 4 linear drives providing two translations and one rotation dof and a serial mechanism allowing a rotation and a translation (see Figure 1 -P representing a Prismatic joint, R a Revolute, U an Universal and S a Spherical joint-). The total number of dof is then equal to 5. The parallel part can be considered as the association of two 2-dof robots that “cooperate” to displace the nacelle (Figure 2). It has been

demonstrated that thanks to the redundancy there is no limitation on the nacelle rotation (no overmobility-type singular position).

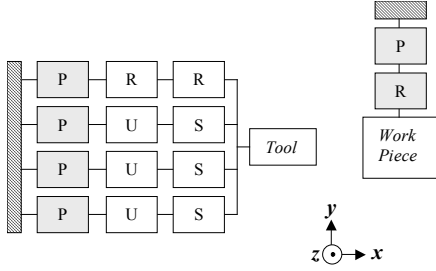


Figure 1: Kinematic representation of ARCHI

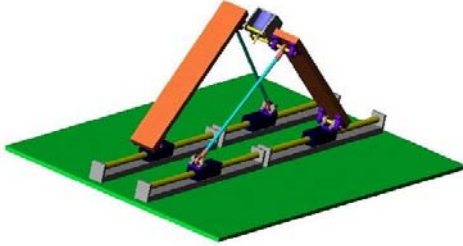


Figure 2: ARCHI CAD view

II.2. Modeling

II.2.1. Position equations

Basic models of ARCHI robot have been yet described in [12]. It has been pointed out that the inverse kinematic model is unique and easy to compute (analytic solution). Concerning the forward kinematic model (FKM), if the robot is perfect, the solution doesn't depend on which set of 3 arms among 4 is selected. Of course, in reality, as the robot is not perfect (errors on arms lengths, offset errors on drives positions...), the solution to the FKM will depend on which non-redundant 3-arm subsystem is considered.

II.2.2. Velocity equation

If $\mathbf{q} = [q_1, q_2, q_3, q_4]^T$ is the vector of drives positions, $\mathbf{x} = [x, y, \theta]^T$ the nacelle configuration described by the position of point C and the nacelle orientation, (x_{12}, y_{12}) and (x_{34}, y_{34}) the coordinates of B_{12} and B_{34} , $\mathbf{v} = [\dot{x}_{12}, \dot{y}_{12}, \dot{x}_{34}, \dot{y}_{34}]^T$ (Figure 3), the velocity equation can be classically written as:

$$\mathbf{J}_v \mathbf{v} = \mathbf{J}_q \dot{\mathbf{q}}$$

with $\mathbf{J}_v, \mathbf{J}_q \in \mathbb{R}^{4 \times 4}$. As $\mathbf{v} = \mathbf{G} \dot{\mathbf{x}}$ ($\mathbf{G} \in \mathbb{R}^{4 \times 3}$), the relation between $\dot{\mathbf{x}}$ and $\dot{\mathbf{q}}$ can be expressed as:

$$\mathbf{J}_x \dot{\mathbf{x}} = \mathbf{J}_q \dot{\mathbf{q}}$$

with $\mathbf{J}_x = \mathbf{J}_v \mathbf{G}$ ($\mathbf{J}_x \in \mathbb{R}^{4 \times 3}$), and if \mathbf{J}_q is not singular:

$$\dot{\mathbf{q}} = \mathbf{J}_m \dot{\mathbf{x}} \quad (1)$$

where:

$$\mathbf{J}_m = \begin{bmatrix} 1 & \frac{y_{12}}{s_1} & d(\sin \theta - \frac{y_{12}}{s_1} \cos \theta) \\ 1 & -\frac{y_{12}}{s_1} & d(\sin \theta + \frac{y_{12}}{s_1} \cos \theta) \\ 1 & \frac{y_{34}}{s_2} & d(-\sin \theta + \frac{y_{34}}{s_2} \cos \theta) \\ 1 & -\frac{y_{34}}{s_2} & d(-\sin \theta - \frac{y_{34}}{s_2} \cos \theta) \end{bmatrix} \in \mathbb{R}^{4 \times 3}$$

$$s_1 = \sqrt{L^2 - y_{12}^2}, \quad s_2 = \sqrt{L^2 - y_{34}^2}$$

For given drives positions eq. (1) is an over-determined linear system of unknown $\dot{\mathbf{x}}$ which least square better solution is:

$$\dot{\mathbf{x}} = \mathbf{J}_m^+ \dot{\mathbf{q}} \quad (2)$$

(+ denotes the pseudo-inversion operator)

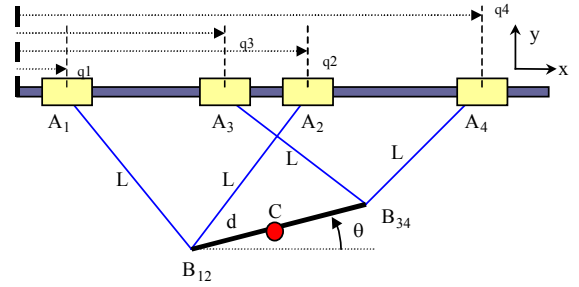


Figure 3: ARCHI parameterization

III. INTERNAL CONSTRAINT MANAGEMENT

Let's consider a m -dof robot actuated by n drives ($n \geq m$) and f the linear application from \mathbb{R}^n to \mathbb{R}^m ($f \in \mathcal{L}(\mathbb{R}^n, \mathbb{R}^m)$) as:

$$\mathbf{F}_{nac} = f(\mathbf{F}_d) \quad (3)$$

where \mathbf{F}_{nac} is the force acting on the nacelle and \mathbf{F}_d drives forces. If $\mathbf{Ker}(f)$ is f null space and $\mathbf{R}(f)$ its range,

$$\dim(\mathbf{Ker}(f)) + \dim(\mathbf{R}(f)) = n$$

and as $\dim(\mathbf{R}(f)) = m$, the dimension of f kernel is then:

$$p = \dim(\mathbf{Ker}(f)) = n - m$$

For a non-redundant robot ($m = n$: f endomorphism), $\mathbf{Ker}(f) = \{\mathbf{0}\}$ and $\forall \mathbf{F}_{nac} \in \mathbb{R}^m, \exists ! \mathbf{F}_d \in \mathbb{R}^n / f(\mathbf{F}_d) = \mathbf{F}_{nac}$.

Otherwise eq. (3) has an infinity of solutions: if $S_{ker} = (F_{S_{ker1}}, \dots, F_{S_{kerp}})$, $1 \leq p \leq n$, is a base of the subspace $Ker(f)$ and \bar{S}_{ker} its complement,

$$\forall F_{nac} \in \mathfrak{R}^m, \exists ! F_{\bar{S}_{ker}} \in \bar{S}_{ker} / f(F_{\bar{S}_{ker}}) = F_{nac}$$

and the solutions of eq. (3) are:

$$F_d = F_{\bar{S}_{ker}} + span(F_{S_{ker1}}, \dots, F_{S_{kerp}}) \quad (4)$$

For any over-actuated mechanism, the relation between F_d and F_{nac} can be expressed by:

$$F_{nac} = f(F_d) = J_m^T F_d, \quad J_m \in \mathfrak{R}^{n \times m} \quad (5)$$

And the solutions of the underdetermined linear system (5) are:

$$F_d = J_m^{T+} F_{nac} + [I - J_m^{T+} J_m^T] F \quad (6)$$

where I is the n -by- n identity matrix and F is any force belonging to \mathfrak{R}^n (the vector $[I - J_m^{T+} J_m^T] F$ corresponds to its projection onto the null-space).

For ARCHI robot $J_m^T \in \mathfrak{R}^{3 \times 4}$ ($n = 4, m = 3$):

$$\dim(R(f)) = rank(J_m) = 3$$

$$\dim(Ker(f)) = 1$$

and consequently eq. (4) can be rewritten as:

$$F_d = F_{\bar{S}_{ker}} + \lambda F_{S_{ker}}, \quad \lambda \in \mathfrak{R} \quad (7)$$

Any value of λ will lead to drives forces reacting against each other and generating internal constraints on the mechanism. It is then necessary to solve eq. (3) taking into account the internal forces acting on the nacelle. The following sections present 3 approaches for drives forces computation managing this internal constraint.

III.1. "Two-arm like" control

In order to solve the underdetermined system, an intuitive idea consists in adding one supplementary equation to the linear system (the dimension of the jacobian kernel is equal to one) that, in static, cancels the compression force acting on the nacelle (Figure 4):

$$(f_1 - f_2) \cdot n = 0 \quad (8)$$

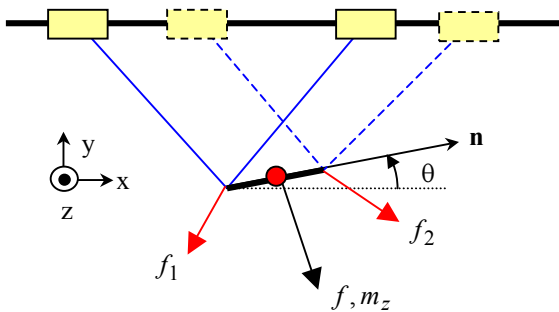


Figure 4: Forces acting on the nacelle

As demonstrated in [12], the constraint expressed by eq. (7) leads to the solution:

$$F_d = J_e \begin{bmatrix} F_{nac} \\ 0 \end{bmatrix} \quad (9)$$

where:

$$J_e = [J_x^{-1} J_q]^T J_f^{-1} \in \mathfrak{R}^{4 \times 4}$$

and:

$$J_f = \begin{bmatrix} 1 & 0 & 1 & 0 \\ 0 & 1 & 0 & 1 \\ d \sin \theta & -d \cos \theta & -d \sin \theta & d \cos \theta \\ \cos \theta & \sin \theta & -\cos \theta & -\sin \theta \end{bmatrix}$$

Of course, it is also possible to set the mechanical constraint acting on the nacelle to a given non-null value in order to eliminate the backlash phenomenon [7]: the computation method keeps unchanged. Basically, this approach is similar to the one proposed by Dauchez [14] for two-arms robots control.

III.2. Minimization of drives Euclidian norm

The force F_d solution of eq. (5) lying into J_m^T kernel is the unique force that minimizes the Euclidian norm of actuators forces:

$$F_d = J_m^{T+} F_{nac} \quad (10)$$

III.3. Minimization of the maximal drive force

The minimization of the maximal drive force is ensured if the infinite norm of actuators forces is minimized. It has been demonstrated that for ARCHI robot the general solution of eq. (5) can be written:

$$F_d = F_{\bar{S}_{ker}} + \lambda F_{S_{ker}}$$

where $\lambda \in \mathfrak{R}$, $F_{\bar{S}_{ker}}$ is the unique solution minimizing the

Euclidian norm of drives forces ($F_{\bar{S}_{ker}} = J_m^{T+} F_{nac}$) and $F_{S_{ker}}$ any force belonging to $ker(J_m^T)$. As the solution corresponding to the minimal infinite norm has necessarily two components equals in absolute value [7]:

$$\begin{aligned} \forall (F_d, F_{nac}) \in \mathfrak{R}^4 \times \mathfrak{R}^3 / \{ J_m^T F_d = F_{nac}, \|F_d\|_{\infty} \text{ minimal} \}, \\ \exists (i, j) \in \{1, \dots, 4\}^2, i \neq j / |F_d(i)| = |F_d(j)| \text{ (i.e. } F_d(i) = \pm F_d(j)) \end{aligned}$$

the set of solutions of the under-determined linear system (5) can then be represented on Figure 5 where each drive force component $F_d(k)$, $k \in \{1, \dots, 4\}$, is plotted as a function of λ (as well as $-F_d(k)$ to find the points corresponding to the condition $F_d(i) = \pm F_d(j)$).

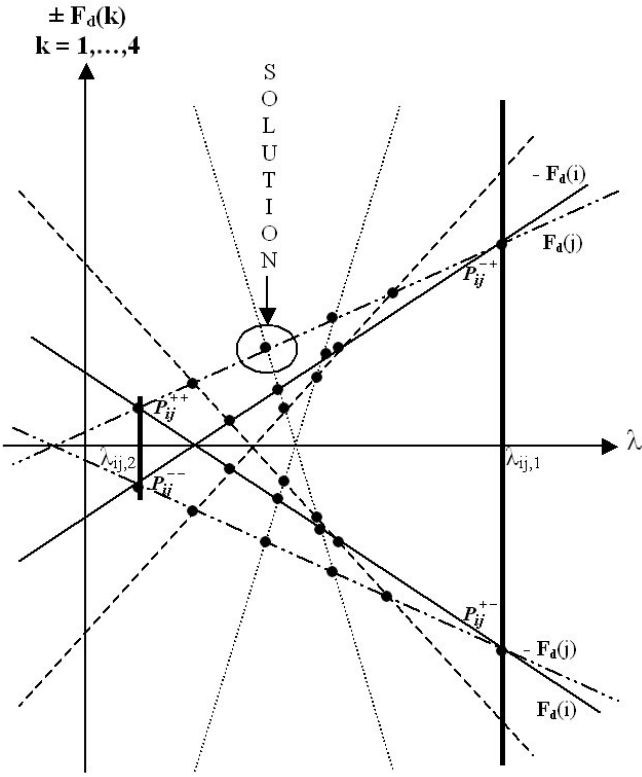


Figure 5. Computation of the minimal drive forces

The $C_8^2 - 4 = 24$ candidate solutions to the minimization problem, depicted on the graph by \bullet (points $P_{ij}^{++}, P_{ij}^{--}, P_{ij}^{+-}, P_{ij}^{-+}, (i, j) \in \{1, \dots, 4\}^2, i \neq j$), correspond to the intersection of two straight lines. Thanks to the symmetry of the graph, only 12 are to be known and considering that the minimal solution can't correspond to the intersection of two lines having slopes of the same sign, only 6 are to be computed. The solution to the minimization problem can then be found among this set of candidate solutions by checking the value of the infinite norm of each one and choosing the minimal. It has to be noticed that this way of solving the minimization problem may be extended to the case of a multi-dimensional null-space.

Summarization of the main steps of the resolution algorithm (Figure 6):

- 1- Computation of $F_{\bar{S}_{ker}}$, unique drive force solution of eq. (5) minimizing F_d Euclidian norm ($F_{\bar{S}_{ker}} = J_m^{T+} F_{nac}$).
- 2- Computation of one force ($F_{S_{ker}}$) belonging to J_m^T null-space by projecting any given Cartesian force belonging to \mathbb{R}^3 on the Jacobian null-space $ker(J_m^T)$ ($F_{S_{ker}} = (I - J_m^{T+} J_m^T) F, F \in \mathbb{R}^3$) or by solving the system $J_m^T F_{S_{ker}} = 0$ setting one component of $F_{S_{ker}}$ to a given value (for example $F_{S_{ker}}(1) = 1$).

- 3- Computation of the scalars $\lambda_{ij,1}, \lambda_{ij,2}$ and of the points $P_{ij}^{++}, P_{ij}^{--}, P_{ij}^{+-}, P_{ij}^{-+}$ (see Figure 5) real candidates, intersections of the straight lines giving each component of drives forces $F_d(k) = \pm(F_{S_{ker}}(k) \lambda + F_{\bar{S}_{ker}}(k))$:

$$\lambda_{ij,1} = \frac{F_d(i) + F_d(j)}{F_{S_{ker}}(i) - F_{S_{ker}}(j)}, \quad \lambda_{ij,2} = \frac{F_d(i) - F_d(j)}{F_{S_{ker}}(i) - F_{S_{ker}}(j)}$$

- 4- Test of this set of candidate solutions to find the one minimizing the maximal drive force.

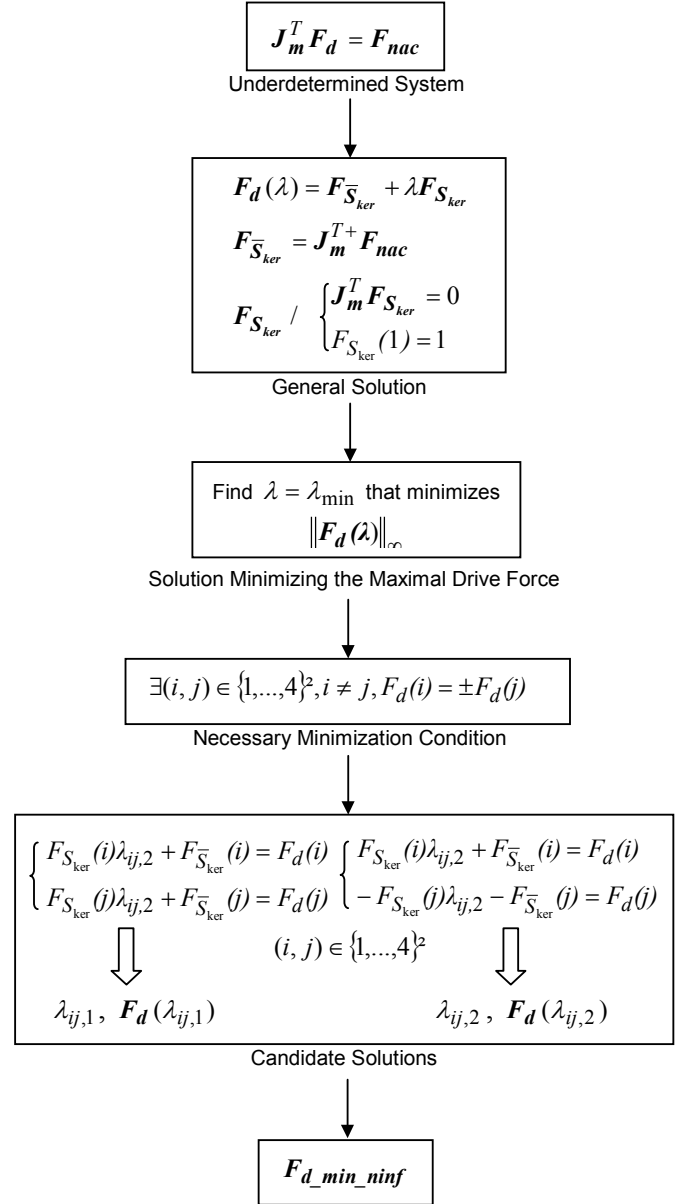


Figure 6. Maximal drive force minimization algorithm

IV. EXPERIMENTATIONS

IV.1. Experimental setup

Robot control task is a RTX (Real Time eXtension) process (implemented in C language) that generates a periodical control task sampled at 2 kHz. User's orders come from the G.U.I (Graphical User Interface, implemented in Visual C++) and are transmitted to the control task through shared memory. An I/O board is a plugged into the computer PCI bus (260 MHz, 64 Mb, running WinNT). The control is ensured by 2 controllers: the first one is a force controller built in the amplifier and the second one a Cartesian Space controller associating a PD controller to one of the drives forces computation algorithms above mentioned. The Figure 7 sums up the robot control:

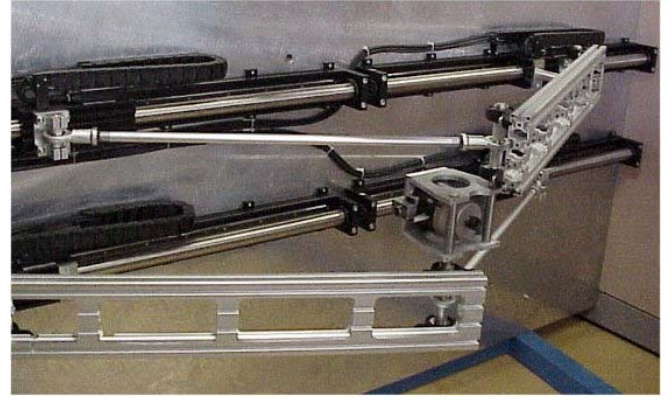


Figure 8. Robot prototype

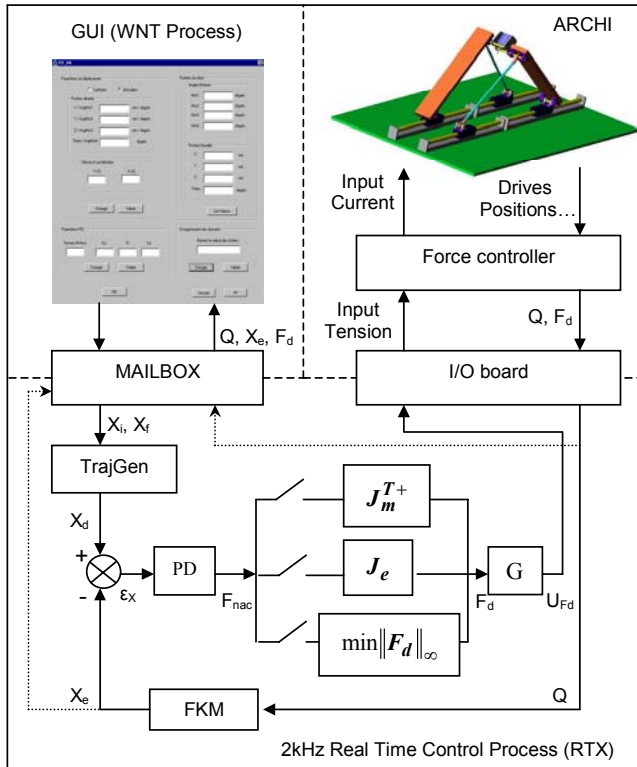


Figure 7. Robot control

IV.2. Prototype

A prototype of the parallel over-actuated sub-mechanism has been built (Figure 8). Its main dimensions and characteristics are:

- Arms length: 0.88 m, nacelle width: 0.11 m
- Brushless Linear Direct Drives maximal velocity: 2.5 m/s, stroke: 0.9 m, maximal force: 750 N, weight: 3.15 Kg

IV.3. Experimental results

The experimental results have been obtained for a 400 ms displacement from the start point $x_i = [0.95 \text{ m}; -0.5 \text{ m}; \pi/2 \text{ rad}]$ to the end point $x_f = [1.35 \text{ m}; -0.65 \text{ m}; 0 \text{ rad}]$ (sine/ramp trajectory generation). The total of moving masses was about 15 Kg. During that motion tracking errors on x and y remain smaller than 2.5 mm and the maximal angular tracking error was lower than $\frac{1}{2}$ degree (Figure 9)¹. The maximal linear drives velocity was above 2 m/s and the corresponding nacelle velocity on x and y was 1.5 m/s whereas the rotation velocity was close to 2 revolutions per second (Figure 10). The nacelle reached a 2 g acceleration (Figure 11).

- Cartesian tracking errors (pseudo-inversion algorithm)

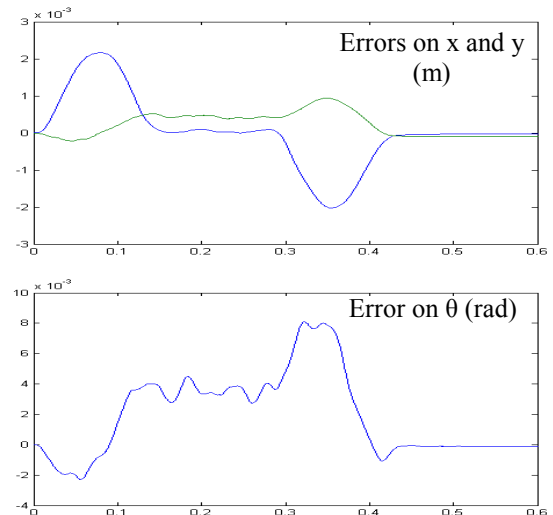


Figure 9: Cartesian errors

¹ In figures 9 to 15, horizontal axis represents Time in (s)

- Cartesian velocities

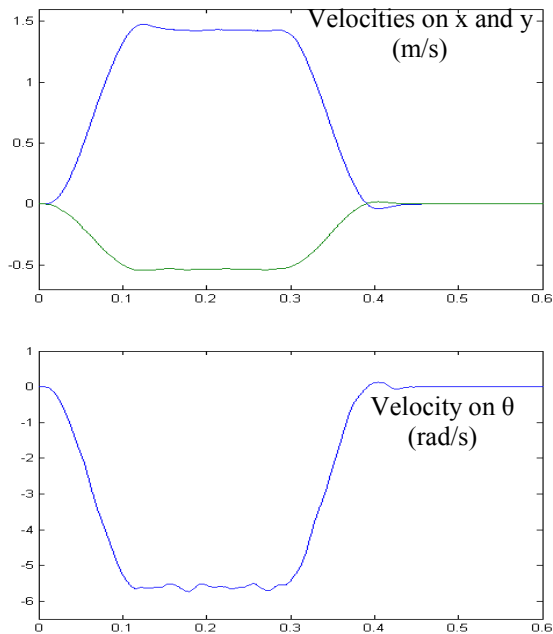


Figure 10: Cartesian velocities

- Cartesian accelerations

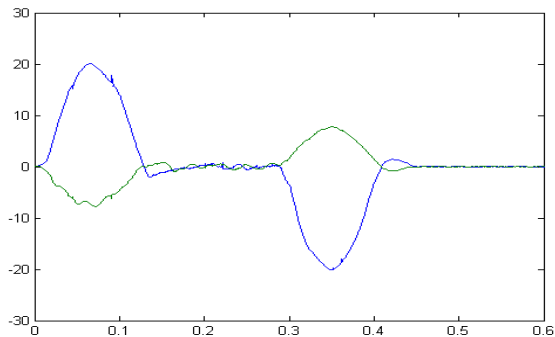


Figure 11: Accelerations on x and y (m/s²)

The following figures describe the evolution of drives forces for each control strategy. During the displacement specified above, the maximal drive force corresponding to the “2-arm like” control was equal to 152 N (Figure 12) whereas in the case of the Euclidian norm minimization it only reached 141 N (Figure 13) and 120 N (Figure 14) when minimizing the infinite norm.

It is then clear that for any robot the control minimizing the infinite norm of drives forces permits to reach higher accelerations and to take the best advantage of drives potentialities (even if it generates drives forces that have no effect on the nacelle force (Figure 15)).

- Actuators forces when selecting the “2-arm like control”

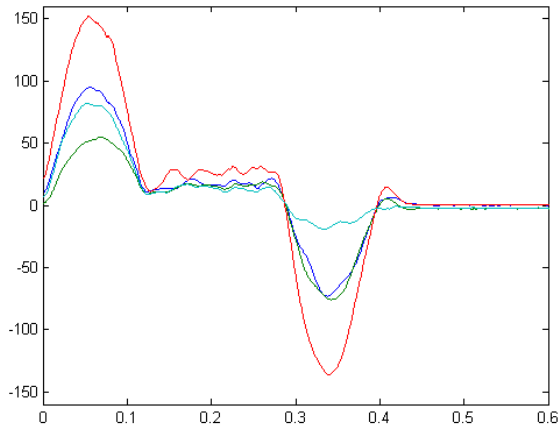


Figure 12. “Two-arm like” control: drives forces (N)

- Actuators forces when minimizing the Euclidian norm

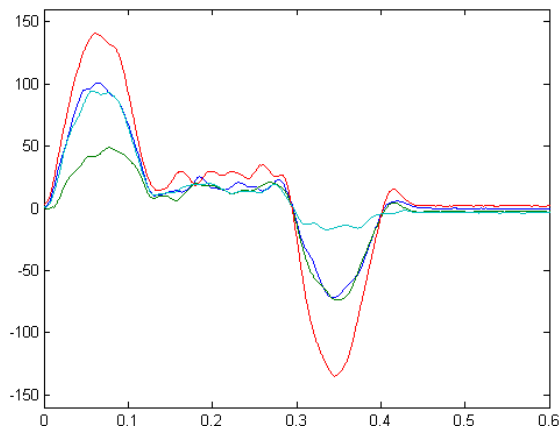


Figure 13. Minimization of the Euclidian norm : drives forces (N)

	No compression	Min. Eucl. norm	Min. Inf. Norm
Max Drive Force	152 N + 8 %	141 N reference	120 N - 15 %

- *Actuators forces when minimizing the infinite norm*

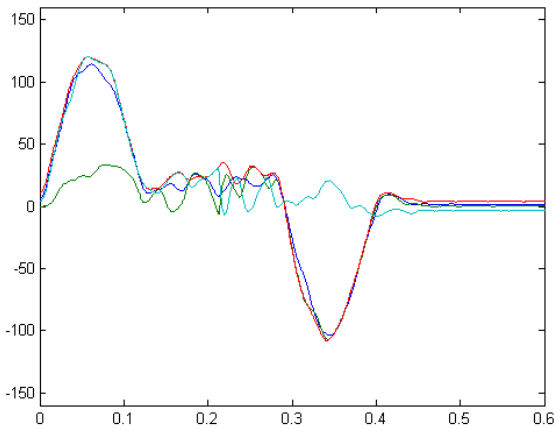


Figure 14. Minimization of the infinite norm: drives forces (N)

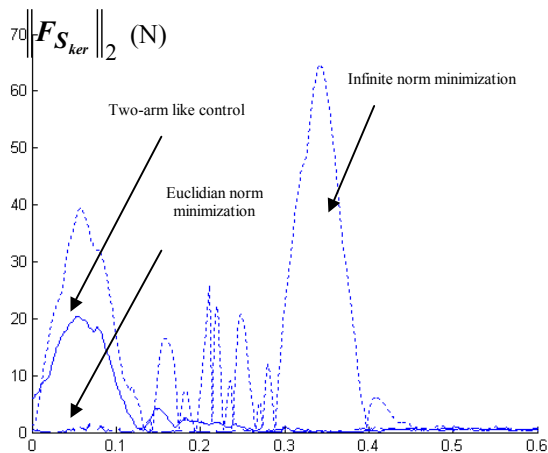


Figure 15. Projection of drives forces on the null-space

V. CONCLUSION

In this paper, several control strategies of a 3-dof over-actuated mechanism have been proposed and tested on a prototype. The “two arm like control” seems to be a good and simple method to cancel out the internal force acting on the nacelle. Methods based on the minimization of the Euclidian norm or the infinite norm of drives forces also proved their efficiency, especially the second one that permits to take the best advantage of actuators potentialities. According to the theory, experimental results have clearly demonstrated the validity and the efficiency of these approaches for controlling over-actuated robots.

REFERENCES

- [1] Clavel R., *Delta, a fast robot with parallel geometry*, 18th International Symposium on Industrial Robots, Lausanne, April 26-28, 1988, pp. 91-100.
- [2] Company O. and Pierrot F., *A new 3T-1R parallel robot*, ICAR '99, International Conference on Advanced Robotics, Tokyo, Japan, October 25-27, 1999, pp. 557-562.
- [3] Pierrot F., Marquet F., Company O., Gil T., *H4 parallel robot: modeling, design and preliminary experiments*. ICRA'2001, Int. Conf. On Robotics and Automation, Seoul, Korea, May 2001.
- [4] Company O., Pierrot F., Launay F., Fiorini C., *Modelling and preliminary design issues of a 3-axis parallel machine-tool*, PKM'2000 (Parallel Kinematics Machines), Ann Arbor, USA, September 13-15, 2000, pp. 14-23.
- [5] Pierrot F., Shibukawa T., *From Hexa to HexaM*. In Proc. IPK'98: Internationales Parallelkinematik-Kolloquium, Zürich, June 4, pp. 75-84, 1998.
- [6] Krut S., Company O., Marquet F., Pierrot F., *Twice: A Tilting Angle Amplification System for Parallel Robots*, ICRA'02, Washington, mai 2002.
- [7] Boulet B., Hayward V., *Robust control of a robot joint with hydraulic actuator redundancy*, ISR'2000, International Symposium on Robotics, Montreal, Canada, may 14-17 2000, pp. 36-41.
- [8] Kock S., Schumacher W., *A mixed elastic and rigid body dynamic model of an actuation redundant parallel robot with high-reduction gears*, ICRA'2000, April 2000.
- [9] Kim J. and Park F.C., *Eclipse – A new parallel mechanism prototype*. Position paper in Proceedings of the First European-American Forum on Parallel Kinematic Machines, Milan, Italy, August 31- September 1, 1998.
- [10] Kim J., Park F.C., Lee J.M., *A new parallel mechanism machine tool capable of five-face machining*. Annals of the CIRP, Vol.48, No.1, pp.337-340, 1999.
- [11] Marquet F., Krut S., Company O., Pierrot, F., *ARCHI, a Redundant Mechanism for Machining with Unlimited Rotation Capacities*, ICAR' 2001, Budapest, August 22-25, 2001, pp. 683-689.
- [12] Marquet F., Krut S., Company O., Pierrot F., *ARCHI: a New Redundant Parallel Mechanism : Modeling, Control and First Results*, IROS'2001, Hawaii, USA, October 29- November 3, 2001.
- [13] Dasgupta B., Mruthyunjaya T.S., *Force redundancy in parallel manipulators: theoretical and practical issues*. Mechanism and Machine Theory, 33(6):727-742, August 1998.
- [14] Dauchez P., Delebarre X., Jourdan R., *Hybrid control of a two-arm robot handling firmly a single rigid object*, Proc. of the 2nd SIFIR, Saragoza, Spain, pp. 67-72, November 1989.

Note: Photos and Videos of ARCHI robot are available at the URL <http://www.lirmm.fr/rdc/pm/archi.html>